Published in final edited form as:
Toxicology. 2015 February 3; 328: 75–81. doi:10.1016/j.tox.2014.12.005.

JNK inhibition of VMAT2 contributes to rotenone-induced oxidative stress and dopamine neuron death

Won-Seok Choi[a,c,1,**], **Hyung-Wook Kim**[b,c,1], and **Zhengui Xia**[c,*]

[a]School of Biological Sciences and Technology, College of Natural Sciences, College of Medicine, Chonnam National University, Gwangju 500-757

[b]College of Life Sciences, Sejong University, Seoul 143-747, Korea

[c]Toxicology Program in the Department of Environmental and Occupational Health Sciences, University of Washington, Seattle, WA 98195

Abstract

Treatment with rotenone, both *in vitro* and *in vivo*, is widely used to model dopamine neuron death in Parkinson's disease upon exposure to environmental neurotoxicants and pesticides. Mechanisms underlying rotenone neurotoxicity are still being defined. Our recent studies suggest that rotenone-induced dopamine neuron death involves microtubule destabilization, which leads to accumulation of cytosolic dopamine and consequently reactive oxygen species (ROS). Furthermore, the c-Jun N-terminal protein kinase (JNK) is required for rotenone-induced dopamine neuron death. Here we report that the neural specific JNK3 isoform of the JNKs, but not JNK1 or JNK2, is responsible for this neuron death in primary cultured dopamine neurons. Treatment with taxol, a microtubule stabilizing agent, attenuates rotenone-induced phosphorylation and presumably activation of JNK. This suggests that JNK is activated by microtubule destabilization upon rotenone exposure. Moreover, rotenone inhibits VMAT2 activity but not VMAT2 protein levels. Significantly, treatment with SP600125, a pharmacological inhibitor of JNKs, attenuates rotenone inhibition of VMAT2. Furthermore, decreased VMAT2 activity following *in vitro* incubation of recombinant JNK3 protein with purified mesencephalic synaptic vesicles suggests that JNK3 can inhibit VMAT2 activity. Together with our previous findings, these results suggest that rotenone induces dopamine neuron death through a series of sequential events including microtubule destabilization, JNK3 activation, VMAT2 inhibition, accumulation of cytosolic dopamine, and generation of ROS. Our data identify JNK3 as a novel regulator of VMAT2 activity.

[*]*Corresponding author at:* Zhengui Xia, Ph.D., Toxicology Program in the Department of Environmental and Occupational Health Sciences, Box 357234, University of Washington, 1959 NE Pacific St. Seattle, Washington, 98195. Tel.: +1 206 616 9433, Fax: 1 206 685 3990. [**]*Corresponding author at:* Won-Seok Choi, Ph.D., School of Biological Sciences and Technology, Chonnam National University, 77 Yonbong-ro, Buk-gu, Gwangju 500-757, Korea. Tel.: +82 62 530, 1912, Fax: +82 62 530 2199.
[1]These authors contributed equally to this work.

Conflict of interest
The authors claim no conflict of interest.

Keywords

Parkinson's disease; rotenone; JNK; dopamine neuron; microtubule; VMAT2

1. Introduction

Parkinson's disease is a common neurodegenerative disorder characterized by selective and progressive loss of dopaminergic neurons in the substantia nigra pars compacta (SNpc) of the midbrain (Olanow and Tatton 1999). Although molecular mechanisms underlying this dopaminergic neuron death are not well understood, one of the long-held theories is that impairment of mitochondrial complex I is a key factor (Abou-Sleiman et al. 2006). However, our recent studies using gene targeting strategy suggest that inhibition of mitochondrial complex I by itself is not sufficient to induce dopamine neuron death (Choi et al. 2008; Choi et al. 2011b).

Most cases of Parkinson's disease are sporadic. Exposure to environmental toxicants including pesticides may increase the risk of developing Parkinson's disease (Costello et al. 2009; Mouradian 2002; Ramsden et al. 2001). Interestingly, administration of rotenone, a natural pesticide widely used worldwide, induces many key features of Parkinson's disease in rodents, including motor deficits, loss of dopaminergic neurons, and the presence of α-synuclein–containing inclusion bodies (Betarbet et al. 2000; Inden et al. 2007; Pan-Montojo et al. 2010; Sherer et al. 2003b). Rotenone is a well-known inhibitor of mitochondrial complex I. A number of studies have suggested that rotenone induces dopamine neuron death by inhibiting mitochondrial complex I activity (Marella et al. 2008; Richardson et al. 2007; Seo et al. 2006; Sherer et al. 2003a; Sherer et al. 2007). However, recent studies using cultured neurons prepared from Ndufs4$^{-/-}$ mouse embryos, which have no detectable complex I activity, questioned this theory (Choi et al. 2008; Choi et al. 2011b). Moreover, alternative mechanisms have been suggested underlying rotenone-induced dopaminergic cell death (Choi et al. 2011b; Ren et al. 2005). Nevertheless, rotenone treatment still provides a useful model to study mechanisms of dopaminergic cell death associated with Parkinson's disease, and it is important to elucidate molecular mechanisms underlying rotenone toxicity.

There is a general consensus that rotenone-induced dopamine neuron death is mediated through oxidative stress (Choi et al. 2011b; Sherer et al. 2002; Sherer et al. 2003a; Sherer et al. 2007; Testa et al. 2005). Activation of the stress-activated JNK, a member of the mitogen-activated protein (MAP) kinases, has also been implicated (Chen et al. 2008; Choi et al. 2010; Kalivendi et al. 2010; Klintworth et al. 2007; Newhouse et al. 2004; Reinhardt et al. 2013). In addition, rotenone causes microtubule destabilization in dopamine neurons, which contributes to rotenone toxicity (Choi et al. 2011b; Ren et al. 2005). We also reported that rotenone-induced microtubule destabilization leads to accumulation of the cytosolic dopamine and ROS (Choi et al. 2011b). However, the signaling pathways leading from microtubule destabilization to accumulation of cytosolic dopamine and oxidative stress have not been identified. In this study, we report that rotenone inhibits the activity of VMAT2, the primary transporter that packages dopamine into presynaptic vesicles in dopamine

neurons (Guillot and Miller 2009). Furthermore, JNK activation occurs downstream from microtubule destabilization, and contributes to VMAT2 inhibition.

2. Materials and Methods

2.1. Animals

Generation and characterization of the JNK3$^{-/-}$ mice was described (Yang et al. 1997). For primary culture, the JNK3 heterozygotes (*JNK3*$^{+/-}$) were bred to generate littermates of *JNK3*$^{+/+}$, *JNK3*$^{+/-}$, and *JNK3*$^{-/-}$ embryos. PCR genotyping of the embryos was performed as described (Yang et al. 1997) and the results were matched to each single embryo culture at the end of the experiment.

2.2. Primary Mesencephalic Neuron Cultures and Drug Treatments

Primary cultured dopamine neurons were prepared from E14 mouse or rat embryos as described (Choi et al. 2010; Choi et al. 2013; Choi et al. 2011a; Choi et al. 2008; Choi et al. 2011b), either as single embryo cultures (for *JNK3*$^{+/+}$ *and JNK3*$^{-/-}$ cultures) or as pooled cultures of C57Bl/6 mouse or Sprague–Dawley rat embryos (Charles Rivers, Wilmington, MA). Briefly, we dissected the mesencephalon of each embryo in phosphate-buffered saline (PBS, pH 7.2, Invitrogen, Carlsbad, CA) on ice. The tissue was washed with Dulbecco's modified Eagle medium (DMEM, Sigma, St Louis, MO) and incubated at 37 °C for 10 min. The medium was replaced with culture media consisting of DMEM supplemented with 4 mM glutamine, 10 mM HEPES buffer, 30 mM glucose, 100 IU/ml penicillin, 0.1 mg/ml streptomycin, and 10% heat-inactivated fetal bovine serum (FBS, Invitrogen). The tissue was then dissociated with a narrow pipet tip (Cat # P-3207, ISC BioExpress, Kaysville, UT) and plated (3–5×10^4 cells/100 μl) on 9-mm diameter Aclar embedding film (Electron Microscopy Sciences, Fort Washington, PA) pre-coated with 100 μg/ml poly-D-lysine and 4 μg/ml laminin (BD Bioscience, Bedford, MA). The cultures were maintained at 37 °C in a humidified 7% CO_2 atmosphere. After overnight incubation, fresh culture media were added. Thereafter, half of the media was changed at every 48 h.

Rotenone and taxol (Sigma) were dissolved in dimethyl sulfoxide (DMSO) as 10 mM stock solutions. Drugs were diluted in N2 media (Invitrogen) right before the drug treatment, and the final concentration of DMSO did not exceed 0.0001%. All drug treatments were performed in defined serum-free N2 medium. Half of the media was replaced with N2 medium on the day before drug treatment, and then again at the time of drug treatment. Cultures treated with vehicle were used as controls.

2.3. Transient transfection of JNK3 plasmid

Primary neurons were cultured from E14 embryos as described above and co-transfected with GFP and JNK3 cDNA or empty vector as a control on DIV5, using FuGENE6 (Life Technologies, Rockville, MD). Two days after the transfection, transfected cells were identified and quantified by GFP autofluorescence. Total GFP+ cells were counted on each coverslip (9mm diameter) and presented as cell number / area.

2.4. siRNA

JNK1, 2 or 3 siRNA and non-silencing siRNA as scrambled control were from Qiagen (Heidelberg, Germany). *Jnk1* siRNA sequence is 5' GAAGCUCAGCCGGCCAUUUdTdT 3'; *Jnk2* siRNA 5' GCCUUGCGCCACCCGUAUAdTdT 3'; *Jnk3* siRNA 5' GCCAGGGACUUGUUGUCAAdTdT 3'; Scrambled siRNA 5' UUCUCCGAACGUGUCACGUdTdT 3' (QIAGEN, Valencia, CA) (Wang et al. 2007). Primary neurons were cultured from E14 Sprague–Dawley rat mesencephalons and plated on the 24-well or 48-well plate. At 80% confluency, cells were transfected with siRNA in combination with ¼ amount of EGFP expression vector using TransMessenger Transfection Reagent (QIAGEN) according to the manufacturer's protocol. The final concentration of siRNAs was 2.5 μg/ml.

2.5. Immunocytochemistry

Cells were fixed with 4% paraformaldehyde /4% sucrose for 30 min at room temperature and incubated for 1 h in blocking buffer (PBS containing 5% BSA, 5% normal goat serum, and 0.1% Triton X-100). The cells were then incubated with primary antibodies in blocking buffer at 4°C overnight. Primary antibodies included mouse monoclonal antibody against tyrosine hydroxylase (TH; 1:500; Sigma), rabbit polyclonal antibody against TH (1:50,000; Pel-Freez, Rogers, AR), rabbit polyclonal antibody against phospho-JNK (1:100; Cell Signaling), and rabbit polyclonal antibody against cleaved caspase 3 (1:1000; Cell Signaling). After three washes with PBS, the cells were incubated at room temperature for one hour with appropriate secondary antibodies: Alexa Fluor 488 (or 568) goat anti-rabbit IgG and Alexa Fluor 568 (or 488) goat anti-mouse IgG (1:200; Molecular Probes, Eugene, OR). Stained cells were monitored under a fluorescence microscope (Leica, Heidelberg, Germany).

2.6. Quantitation of TH^+ or Total Neurons

Cells immunostained positive for TH antibody and having neurites twice the length of the soma were scored as TH^+ cells. All TH^+ cells on a 9-mm diameter Aclar embedding film were scored.

2.7. Preparation of free and complex tubulin

Free or polymerized tubulin was extracted from cells as described (Choi et al. 2011a; Jiang et al. 2006). Briefly, cells were maintained in 24-well plates and washed twice at 37 °C with 1 ml of Buffer A (0.1 M MES (pH 6.75), 1 mM MgSO4, 2 mM EGTA, 0.1 mM EDTA, and 4 M glycerol). The cells were then incubated at 37 °C for 5 min in 300 μl of free tubulin extraction buffer (Buffer A plus 0.1% (v/v) Triton X-100 and protease inhibitors). The extracts were removed and centrifuged at 37 °C for 2 min at 16000 × g. The supernatant fractions were used as free cytosolic tubulin samples. The pellet fractions and cells remaining in the culture dish were dissolved in 600 μl of 25 mM Tris (pH 6.8) plus 0.5% SDS and used as polymerized tubulin samples. Equal amounts of protein from free or polymerized tubulin samples were analyzed by immunoblotting with anti-α-tubulin antibody.

2.8. Immunoblot analysis

Protein lysates were analyzed by SDS-PAGE gel electrophoresis and immunoblotting as described (Choi et al. 2010). Antibodies against α-tubulin and synaptophysin were purchased from Sigma. Anti-VMAT2 antibody was from Novus (Littleton, CO).

2.9. ROS labeling and quantification

Cells were incubated at 37°C for 15 min with CM-DCFDA (5 μM 5-(and-6)-chloromethyl-2', 7'-dichlorodihydrofluorescein diacetate acetyl ester, Molecular Probes), washed, and then incubated in pre-warmed PBS at 37°C for 15 minutes. The images of 8 fields from each well were photographed with a fluorescence microscope equipped with a temperature-controlled stage at 37°C (Nikon). Cells were then fixed with 4% paraformaldehyde immediately and processed for immunostaining for TH. The images from the same 8 fields were digitalized and compared after staining. The staining intensity of CM-DCFDA dye (ROS) in the TH^+ neurons was quantified using NIH ImageJ program (http://rsb.info.nih.gov/ij/). All TH^+ neurons in captured images were analyzed and the average level of ROS per TH^+ neuron was calculated.

2.10. Preparation of synaptic vesicles and in vitro VMAT2 activity assay

Synaptic vesicles were isolated using synaptic vesicle isolation kit (Sigma) and quantified using the bicinchoninic assay (Pierce Chemical, Waltham, MA). Uptake of dopamine was measured by incubating synaptic vesicles with [^{3}H]dopamine (20–40 Ci/mmol, PerkinElmer) in assay buffer (10 mM Potassium Phosphate, pH 7.4, 110 mM KCl, 1 mM MgCl2, 2 mM K-ATP) for 2 min. The mixture was filtered through GF/C filter (Millipore, Billerica, MA), and quantified by liquid scintillation counting (Ho and Blum 1998). Uptake rate was calculated as [3H]dopamine (pmol) / synaptic vesicle (mg) / min then presented as percent activity over control. Recombinant JNK3 protein was from Millipore.

2.11. Statistical Analysis

Data were from at least three independent experiments, each with at least duplicate or triplicate determinations. Statistical analysis of data was performed using one-way ANOVA and post-hoc Student's *t* test. Error bars represent standard error of means (SEM). * $p<0.05$; ** $p<0.01$; *** $p < 0.005$; ns, not statistically significant.

3. Results

3.1. The neural specific JNK3 isoform, but not JNK1 or JNK2, contributes to rotenone-induced dopamine neuron death

There are three JNK isoforms (Weston and Davis 2007). We reported that the neural specific JNK3 is required for dopamine neuron death upon rotenone treatment (Choi et al. 2010). Here, we treated primary dopamine neurons cultured from E14 mouse mesencephalon with rotenone for 8 h, and confirmed that rotenone induces phosphorylation of JNK, monitored by immunostaining using an anti-phospho-JNK antibody that specifically recognizes the phosphorylated and activated JNK (Fig. 1 *A*). Dopamine neurons were identified by immunostaining for tyrosine hydroxylase (TH), the rate-limiting enzyme in dopamine

synthesis and a marker for dopaminergic neurons. TH^+ dopaminergic neurons from $JNK3^{-/-}$ mice were more resistant to rotenone toxicity (Fig. 1B), consistent with our previous report (Choi et al. 2010). There were significantly fewer GFP^+ cells co-transfected with JNK3 cDNA than those with control vector at 48 h post transfection (Fig. 1, C and D). However, we observed similar number of GFP^+ cells in either JNK3 expression vector or control vector transfected samples at 24 h post transfection (data not shown), suggesting equivalent transfection efficiency. Furthermore the morphology of JNK3 transfected cells was typically unhealthy in contrast to the control (Fig 1C). These data suggest that ectopic expression of JNK3 is sufficient to induce cell death in primary mesencephalic cultures.

To further elucidate molecular mechanisms of rotenone toxicity, we investigated the contribution of JNK1 and JNK2. Mesencephalic neuron cultures were transfected with control or siRNAs specific for JNK1, 2 or 3. Rotenone-induced dopaminergic neuron death was specifically prevented by JNK3 siRNA but not by either JNK1 or JNK2 siRNA (Fig. 2). These data demonstrate that JNK3, but not JNK1 or JNK2, mediates rotenone-induced dopaminergic neuron death.

3.2. JNK3 contributes to ROS generation and caspase activation in dopamine neurons upon rotenone treatment

Rotenone induces dopamine neuron death through ROS production (Choi et al. 2011b) and caspase 3 activation (Choi et al. 2010). To investigate the role of JNK3 in this process, we measured ROS and caspase activation in $Jnk3^{+/+}$ and $Jnk3^{-/-}$ dopamine neurons after rotenone treatment. ROS production was measured by CM-DCFDA staining in live cells, which were later matched to TH immunostaining. ROS production was increased in $Jnk3^{+/+}$ dopamine neurons upon rotenone treatment, but the ROS increase was greatly attenuated in $Jnk3^{-/-}$ neurons (Fig. 3). Similarly, rotenone increased the number of active caspase 3^+, dopamine neurons cultured from $Jnk3^{+/+}$ mouse embryos (Fig. 4), indicating that rotenone induces activation of caspase 3 and apoptosis. However, this caspase 3 activation was significantly reduced in $Jnk3^{-/-}$ neurons. Thus, JNK3 is required for rotenone-induced ROS production and apoptosis of dopamine neurons.

3.3. JNK is activated by microtubule destabilization

Previously, we demonstrated that rotenone induces microtubule depolymerization, followed by accumulation of cytosolic dopamine and ROS that lead to dopaminergic neuron death (Choi et al. 2011b). Data in Fig. 5A show the time course of free tubulin accumulation upon rotenone treatment of mesencephalic neuron cultures. Because rotenone-induced ROS production and dopamine neuron death require both microtubule destabilization and JNK activation, we hypothesized that microtubule depolymerization may activate JNK. Indeed, pretreatment with taxol, a microtubule stabilizer, decreased rotenone-induced JNK activation in dopamine neurons (Fig. 5B), suggesting that JNK is activated by microtubule destabilization.

3.4. Rotenone inhibits VMAT2 activity in a JNK-dependent manner

We reported that rotenone specifically increases cytosolic but not vesicular dopamine (Choi et al. 2011b). In addition, adenovirus expressing VMAT2 inhibits rotenone-induced TH^+

neuron death (Choi et al. 2011b). Because VMAT2 is the primary transporter that packages dopamine into presynaptic vesicles in dopamine neurons (Guillot and Miller 2009), we hypothesized that rotenone disrupts VMAT2 function, either by inhibiting its activity or expression, thereby leading to the accumulation of cytoplasmic dopamine.

To determine the effect of rotenone on VMAT2 activity or expression, we utilized the human dopaminergic SH-SY5Y cells to facilitate biochemical analysis because primary mesencephalic neuron culture preparations only contain 1–3% TH^+ dopaminergic neurons. SH-SY5Y cells are sensitive to rotenone and commonly used for mechanistic studies of dopamine neuron death (Klintworth et al. 2007). SH-SY5Y cells were treated with 0.4 μM rotenone for 0, 2, 4, or 8 h, time points before cell death was detectable (data not shown). Synaptic vesicles were isolated from these cells and subjected to dopamine reuptake assay or Western analysis. Rotenone treatment for 8 h significantly inhibited VMAT2 activity (Fig. 6A) but had no effect on VMAT2 protein level (Fig. 6B). Interestingly, pretreatment with SP600125, a pharmacological inhibitor of JNKs, significantly attenuated the inhibitory effect of rotenone on VMAT2 activity (Fig. 6C). Finally, direct incubation of synaptic vesicles, isolated from striatum of C57BL/6 mice, with purified recombinant JNK3 protein was sufficient to inhibit VMAT2 activity *in vitro* (Fig. 6D). Similar results were obtained when synaptic vesicles were purified from primary cultured dopaminergic neurons (Fig. 6E). These data suggest that rotenone-induced dopamine neuron death may involve JNK inhibition of VMAT2 activity.

4. Discussion

Treatment with rotenone is a valuable experimental model to study how environmental exposure to neurotoxicants may cause dopamine neuron death associated with Parkinson's disease. The goal of this study is to further elucidate signaling mechanisms responsible for rotenone-induced dopamine neuron death.

Rotenone toxicity to dopamine neurons is due to accumulation of cytosolic but not vesicular dopamine (Choi et al. 2011b). Cytosolic dopamine is subject to oxidation which causes oxidative stress (Choi et al. 2011b; Hastings et al. 1996). To understand how rotenone increases cytosolic dopamine, we examined the effect of rotenone on the activity and protein level of VMAT2. Our data suggest that rotenone inhibits the activity of VMAT2 without affecting its protein level. These results are consistent with the notion that VMAT2 is protective for while loss of VMAT2 function is detrimental to dopamine neurons (Guillot and Miller 2009; Taylor et al. 2011).

Because microtubule-depolymerizing agents such as colchicine or nocodazole activate JNK (Ren et al. 2009), we investigated if the two mechanisms responsible for rotenone-induced dopamine neuron death, JNK activation and microtubule destabilization, are interrelated. Several lines of evidence presented in this study suggest that rotenone-induced JNK activation is downstream from microtubule destabilization, but upstream of accumulation of cytosolic dopamine and ROS. First, taxol, a microtubule stabilizing agent that suppresses rotenone-induced dopamine neuron death (Choi et al. 2011b), inhibits phosphorylation of JNK upon rotenone treatment, suggesting that microtubule destabilization causes JNK

activation. Secondly, pharmacological inhibition of JNKs attenuates the effect of rotenone on VMAT2 inhibition. *Jnk3*-null dopamine neurons are more resistant to ROS production and caspase activation by rotenone treatment. These results place JNK activation upstream of ROS and dopamine accumulation. Interestingly, previous reports suggest that JNK is activated by ROS in neurons (Choi et al. 2011b; Choi et al. 1999; Shiah et al. 1999; Xu et al. 2002). We report here that JNK activation can also trigger ROS production. We hypothesize that activated JNK inhibits VMAT2, leading to ROS production, which in turn further reinforces JNK activation, resulting in a positive feedback loop.

JNK has been implicated in dopamine neuron death in multiple Parkinson's disease models (Junn and Mouradian 2001; Klintworth et al. 2007; Newhouse et al. 2004; Peng et al. 2004; Saporito et al. 1999). Three distinct genes, *jnk1*, *jnk2*, and *jnk3*, have been identified to encode JNKs (Gupta et al. 1996). In contrast to JNK1 and JNK2, which are widely expressed in a variety of tissues, JNK3 is only expressed in the brain and to a much lesser extent in the heart and testis (Mohit et al. 1995). Previously we demonstrated the JNK3 isoform as a common cell death mediator in dopamine neurons treated with paraquat or rotenone (Choi et al. 2010). In this study, we used RNAi technology to block the function of the three JNK isoforms respectively. Our data show that JNK3, but not JNK1 or JNK2, is critical for rotenone-induced dopamine neuron death. This result also indicates that JNK inhibition of VMAT2 is likely mediated by the JNK3 isoform. This notion is further strengthened by the finding that purified, recombinant JNK3 protein is sufficient to inhibit VMAT2 activity in a reconstituted *in vitro* system.

In summary, in combination with our previous findings (Choi et al. 2011b), the data presented here identify VMAT2 inhibition and ROS production as a novel mechanism by which JNK activation, downstream of microtubule depolymerization upon rotenone treatment, induces dopamine neuron death (Fig. 6F).

Supplementary Material

Refer to Web version on PubMed Central for supplementary material.

Acknowledgements

This work was financially supported by Basic Science Research Program through the National Research Foundation of Korea (NRF) funded by the Ministry of Science, ICT & Future Planning [2013R1A1A1059258 to WSC], and by National Institutes of Health (NIH) grant [ES012215 to ZX].

References

Abou-Sleiman PM, Muqit MM, Wood NW. Expanding insights of mitochondrial dysfunction in Parkinson's disease. Nat Rev Neurosci. 2006; 7:207–219. [PubMed: 16495942]

Betarbet R, Sherer TB, MacKenzie G, Garcia-Osuna M, Panov AV, Greenamyre JT. Chronic systemic pesticide exposure reproduces features of Parkinson's disease. Nat Neurosci. 2000; 3:1301–1306. [PubMed: 11100151]

Chen S, Zhang X, Yang D, Du Y, Li L, Li X, Ming M, Le W. D2/D3 receptor agonist ropinirole protects dopaminergic cell line against rotenone-induced apoptosis through inhibition of caspase- and JNK-dependent pathways. FEBS Lett. 2008; 582:603–610. [PubMed: 18242171]

Choi WS, Abel G, Klintworth H, Flavell RA, Xia Z. JNK3 mediates paraquat- and rotenone-induced dopaminergic neuron death. J Neuropathol Exp Neurol. 2010; 69:511–520. [PubMed: 20418776]

Choi WS, Kim HW, Xia Z. Preparation of primary cultured dopaminergic neurons from mouse brain. Methods Mol Biol. 2013; 1018:61–69. [PubMed: 23681617]

Choi WS, Klintworth HM, Xia Z. JNK3-mediated apoptotic cell death in primary dopaminergic neurons. Methods Mol Biol. 2011a; 758:279–292. [PubMed: 21815073]

Choi WS, Kruse SE, Palmiter RD, Xia Z. Mitochondrial complex I inhibition is not required for dopaminergic neuron death induced by rotenone, MPP+, or paraquat. Proc Natl Acad Sci U S A. 2008; 105:15136–15141. [PubMed: 18812510]

Choi WS, Palmiter RD, Xia Z. Loss of mitochondrial complex I activity potentiates dopamine neuron death induced by microtubule dysfunction in a Parkinson's disease model. J Cell Biol. 2011b; 192:873–882. [PubMed: 21383081]

Choi WS, Yoon SY, Oh TH, Choi EJ, O'Malley KL, Oh YJ. Two distinct mechanisms are involved in 6-hydroxydopamine- and MPP+- induced dopaminergic neuronal cell death: role of caspases, ROS, and JNK. J Neurosci Res. 1999; 57:86–94. [PubMed: 10397638]

Costello S, Cockburn M, Bronstein J, Zhang X, Ritz B. Parkinson's disease and residential exposure to maneb and paraquat from agricultural applications in the central valley of California. Am J Epidemiol. 2009; 169:919–926. [PubMed: 19270050]

Guillot TS, Miller GW. Protective actions of the vesicular monoamine transporter 2 (VMAT2) in monoaminergic neurons. Mol Neurobiol. 2009; 39:149–170. [PubMed: 19259829]

Gupta S, Barrett T, Whitmarsh AJ, Cavanagh J, Sluss HK, Derijard B, Davis RJ. Selective interaction of JNK protein kinase isoforms with transcription factors. EMBO J. 1996; 15:2760–2770. [PubMed: 8654373]

Hastings TG, Lewis DA, Zigmond MJ. Role of oxidation in the neurotoxic effects of intrastriatal dopamine injections. Proc Natl Acad Sci U S A. 1996; 93:1956–1961. [PubMed: 8700866]

Ho A, Blum M. Induction of interleukin-1 associated with compensatory dopaminergic sprouting in the denervated striatum of young mice: model of aging and neurodegenerative disease. J Neurosci. 1998; 18:5614–5629. [PubMed: 9671653]

Inden M, Kitamura Y, Takeuchi H, Yanagida T, Takata K, Kobayashi Y, Taniguchi T, Yoshimoto K, Kaneko M, Okuma Y, Taira T, Ariga H, Shimohama S. Neurodegeneration of mouse nigrostriatal dopaminergic system induced by repeated oral administration of rotenone is prevented by 4-phenylbutyrate, a chemical chaperone. J Neurochem. 2007; 101:1491–1504. [PubMed: 17459145]

Jiang Q, Yan Z, Feng J. Neurotrophic factors stabilize microtubules and protect against rotenone toxicity on dopaminergic neurons. J Biol Chem. 2006; 281:29391–29400. [PubMed: 16887804]

Junn E, Mouradian MM. Apoptotic signaling in dopamine-induced cell death: the role of oxidative stress, p38 mitogen-activated protein kinase, cytochrome c and caspases. J Neurochem. 2001; 78:374–383. [PubMed: 11461973]

Kalivendi SV, Yedlapudi D, Hillard CJ, Kalyanaraman B. Oxidants induce alternative splicing of alpha-synuclein: Implications for Parkinson's disease. Free Radic Biol Med. 2010; 48:377–383. [PubMed: 19857570]

Klintworth H, Newhouse K, Li T, Choi WS, Faigle R, Xia Z. Activation of c-Jun N-Terminal Protein Kinase Is a Common Mechanism Underlying Paraquat- and Rotenone-Induced Dopaminergic Cell Apoptosis. Toxicol Sci. 2007; 97:149–162. [PubMed: 17324951]

Marella M, Seo BB, Nakamaru-Ogiso E, Greenamyre JT, Matsuno-Yagi A, Yagi T. Protection by the NDI1 gene against neurodegeneration in a rotenone rat model of Parkinson's disease. PLoS One. 2008; 3:e1433. [PubMed: 18197244]

Mohit AA, Martin JH, Miller CA. p493F12 kinase: a novel MAP kinase expressed in a subset of neurons in the human nervous system. Neuron. 1995; 14:67–78. [PubMed: 7826642]

Mouradian MM. Recent advances in the genetics and pathogenesis of Parkinson disease. Neurology. 2002; 58:179–185. [PubMed: 11805242]

Newhouse K, Hsuan SL, Chang SH, Cai B, Wang Y, Xia Z. Rotenone-Induced Apoptosis Is Mediated by p38 and JNK MAP Kinases in Human Dopaminergic SH-SY5Y Cells. Toxicol. Sci. 2004; 79:137–146. [PubMed: 14976342]

Olanow CW, Tatton WG. Etiology and pathogenesis of Parkinson's disease. Annu Rev Neurosci. 1999; 22:123–144. [PubMed: 10202534]

Pan-Montojo F, Anichtchik O, Dening Y, Knels L, Pursche S, Jung R, Jackson S, Gille G, Spillantini MG, Reichmann H, Funk RH. Progression of Parkinson's disease pathology is reproduced by intragastric administration of rotenone in mice. PLoS One. 2010; 5:e8762. [PubMed: 20098733]

Peng J, Mao XO, Stevenson FF, Hsu M, Andersen JK. The herbicide paraquat induces dopaminergic nigral apoptosis through sustained activation of the JNK pathway. J Biol Chem. 2004; 279:32626–32632. [PubMed: 15155744]

Ramsden DB, Parsons RB, Ho SL, Waring RH. The aetiology of idiopathic Parkinson's disease. Mol Pathol. 2001; 54:369–380. [PubMed: 11724911]

Reinhardt P, Schmid B, Burbulla LF, Schondorf DC, Wagner L, Glatza M, Hoing S, Hargus G, Heck SA, Dhingra A, Wu G, Muller S, Brockmann K, Kluba T, Maisel M, Kruger R, Berg D, Tsytsyura Y, Thiel CS, Psathaki OE, Klingauf J, Kuhlmann T, Klewin M, Muller H, Gasser T, Scholer HR, Sterneckert J. Genetic correction of a LRRK2 mutation in human iPSCs links parkinsonian neurodegeneration to ERK-dependent changes in gene expression. Cell Stem Cell. 2013; 12:354–367. [PubMed: 23472874]

Ren Y, Jiang H, Yang F, Nakaso K, Feng J. Parkin Protects Dopaminergic Neurons against Microtubule-depolymerizing Toxins by Attenuating Microtubule-associated Protein Kinase Activation. J Biol Chem. 2009; 284:4009–4017. [PubMed: 19074146]

Ren Y, Liu W, Jiang H, Jiang Q, Feng J. Selective vulnerability of dopaminergic neurons to microtubule depolymerization. J Biol Chem. 2005; 280:34105–34112. [PubMed: 16091364]

Richardson JR, Caudle WM, Guillot TS, Watson JL, Nakamaru-Ogiso E, Seo BB, Sherer TB, Greenamyre JT, Yagi T, Matsuno-Yagi A, Miller GW. Obligatory role for complex I inhibition in the dopaminergic neurotoxicity of 1-methyl-4-phenyl-1,2,3,6-tetrahydropyridine (MPTP). Toxicol Sci. 2007; 95:196–204. [PubMed: 17038483]

Saporito MS, Brown EM, Miller MS, Carswell S. -CEP-1347/KT-7515, an inhibitor of c-jun N-terminal kinase activation, attenuates the 1-methyl-4-phenyl tetrahydropyridine-mediated loss of nigrostriatal dopaminergic neurons In vivo. J Pharmacol Exp Ther. 1999; 288:421–427. [PubMed: 9918541]

Seo BB, Nakamaru-Ogiso E, Flotte TR, Matsuno-Yagi A, Yagi T. In vivo complementation of complex I by the yeast Ndi1 enzyme. Possible application for treatment of Parkinson disease. J Biol Chem. 2006; 281:14250–14255. [PubMed: 16543240]

Sherer TB, Betarbet R, Stout AK, Lund S, Baptista M, Panov AV, Cookson MR, Greenamyre JT. An in vitro model of Parkinson's disease: linking mitochondrial impairment to altered alphasynuclein metabolism and oxidative damage. J Neurosci. 2002; 22:7006–7015. [PubMed: 12177198]

Sherer TB, Betarbet R, Testa CM, Seo BB, Richardson JR, Kim JH, Miller GW, Yagi T, Matsuno-Yagi A, Greenamyre JT. Mechanism of toxicity in rotenone models of Parkinson's disease. J Neurosci. 2003a; 23:10756–10764. [PubMed: 14645467]

Sherer TB, Kim JH, Betarbet R, Greenamyre JT. Subcutaneous Rotenone Exposure Causes Highly Selective Dopaminergic Degeneration and alpha-Synuclein Aggregation. Exp. Neurol. 2003b; 179:9–16. [PubMed: 12504863]

Sherer TB, Richardson JR, Testa CM, Seo BB, Panov AV, Yagi T, Matsuno-Yagi A, Miller GW, Greenamyre JT. Mechanism of toxicity of pesticides acting at complex I: relevance to environmental etiologies of Parkinson's disease. J Neurochem. 2007; 100:1469–1479. [PubMed: 17241123]

Shiah SG, Chuang SE, Chau YP, Shen SC, Kuo ML. Activation of c-Jun NH2-terminal kinase and subsequent CPP32/Yama during topoisomerase inhibitor beta-lapachone-induced apoptosis through an oxidation-dependent pathway. Cancer Res. 1999; 59:391–398. [PubMed: 9927052]

Taylor TN, Caudle WM, Miller GW. VMAT2-Deficient Mice Display Nigral and Extranigral Pathology and Motor and Nonmotor Symptoms of Parkinson's Disease. Parkinsons Dis. 2011; 2011:124165. [PubMed: 21403896]

Testa CM, Sherer TB, Greenamyre JT. Rotenone induces oxidative stress and dopaminergic neuron damage in organotypic substantia nigra cultures. Brain Res Mol Brain Res. 2005; 134:109–118. [PubMed: 15790535]

Wang Y, Luo W, Reiser G. Proteinase-activated receptor-1 and -2 induce the release of chemokine GRO/CINC-1 from rat astrocytes via differential activation of JNK isoforms, evoking multiple protective pathways in brain. Biochem J. 2007; 401:65–78. [PubMed: 16942465]

Weston CR, Davis RJ. The JNK signal transduction pathway. Curr Opin Cell Biol. 2007; 19:142–149. [PubMed: 17303404]

Xu J, Kao SY, Lee FJ, Song W, Jin LW, Yankner BA. Dopamine-dependent neurotoxicity of alpha-synuclein: a mechanism for selective neurodegeneration in Parkinson disease. Nat Med. 2002; 8:600–606. [PubMed: 12042811]

Yang DD, Kuan CY, Whitmarsh AJ, Rincon M, Zheng TS, Davis RJ, Rakic P, Flavell RA. Absence of excitotoxicity-induced apoptosis in the hippocampus of mice lacking the Jnk3 gene. Nature. 1997; 389:865–870. [PubMed: 9349820]

Highlights

JNK3 is responsible for rotenone-induced death of primary cultured dopamine neurons.

JNK is activated by microtubule destabilization upon rotenone exposure.

ROS and caspase activation is mediated by JNK3 in rotenone-induced dopaminergic neuron death.

We identify JNK3 as a novel regulator of VMAT2 activity.

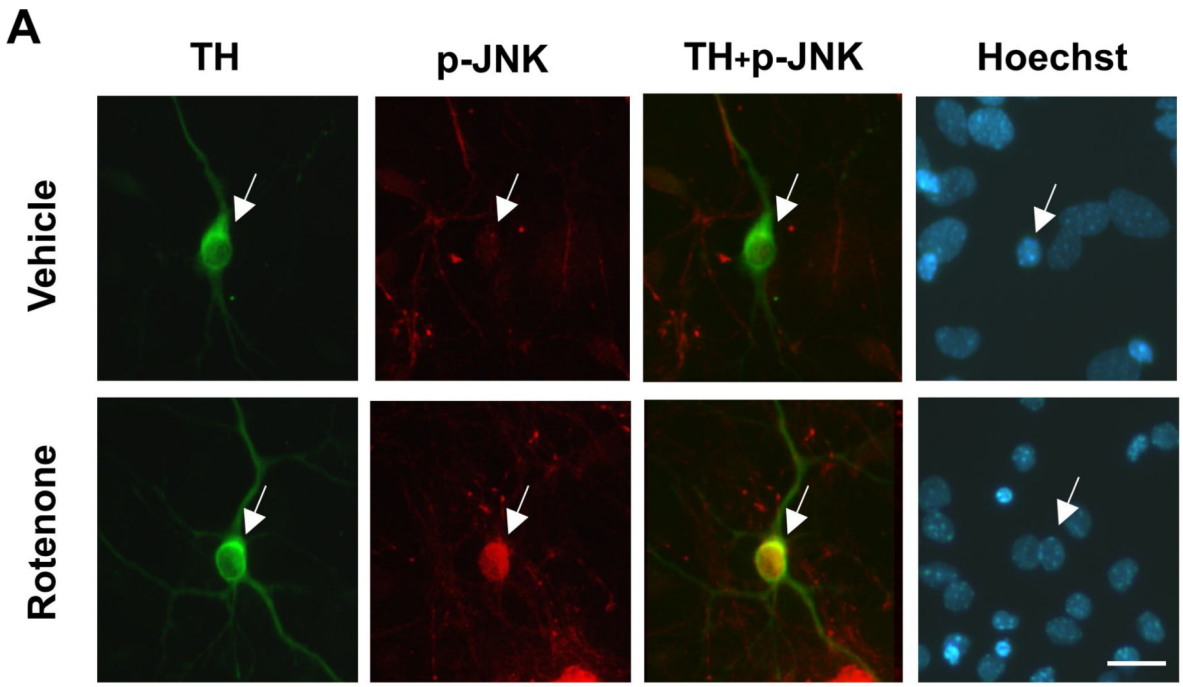

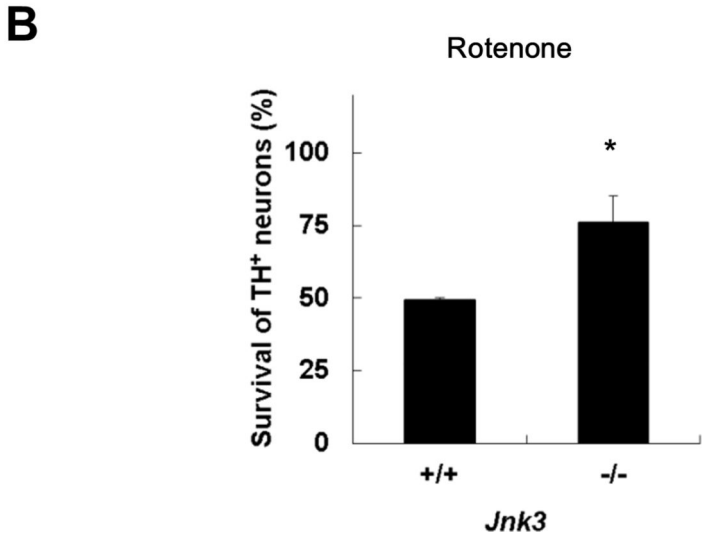

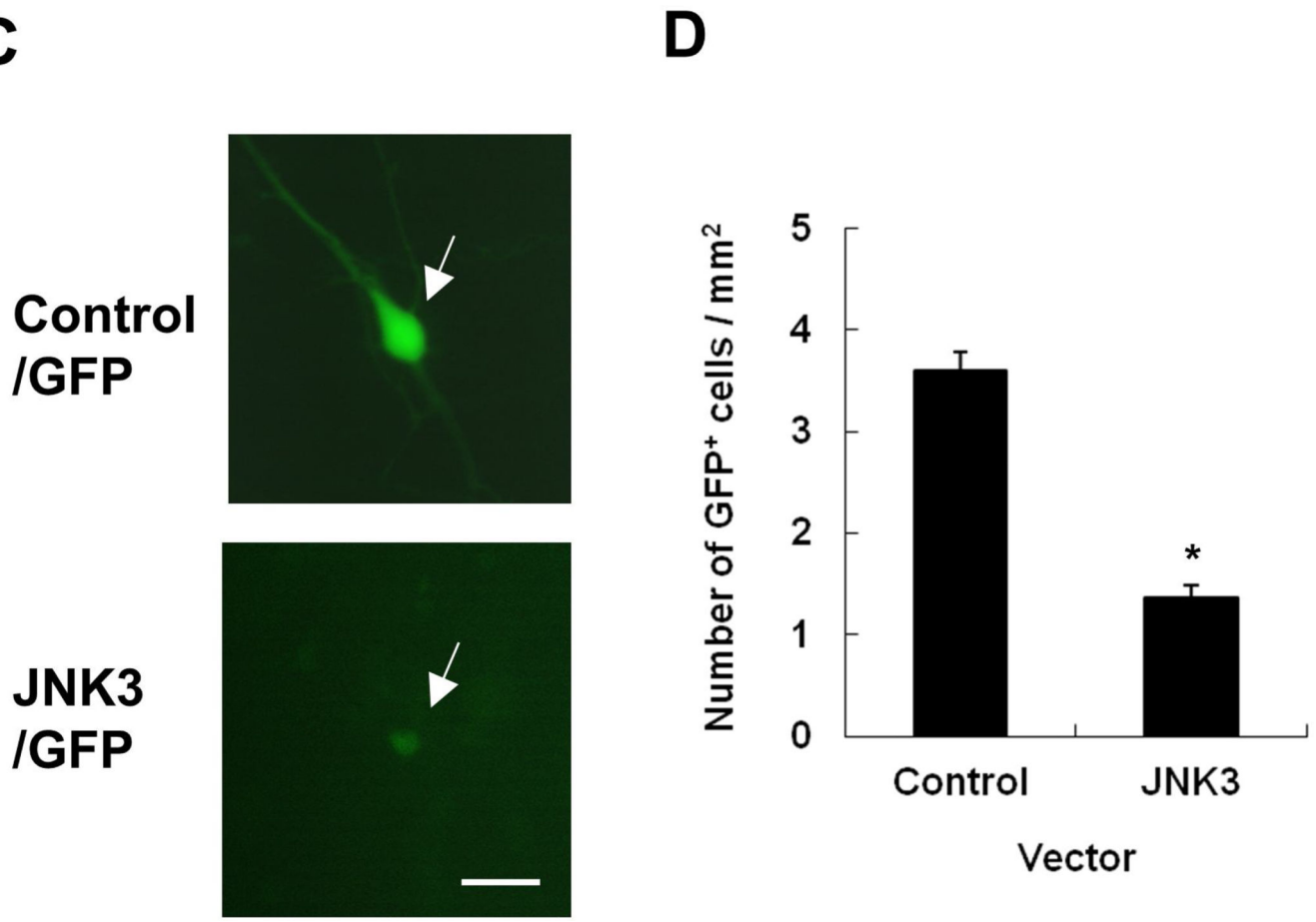

Fig. 1. Rotenone-induced dopamine neuron death requires the function of JNK3, a neural specific JNK isoform

(A) Primary ventral mesencephalic cultures were prepared from embryonic day (E) 14 wild type C57BL/6 mice. After 6 days *in vitro* (DIV6), cultures were treated with 5 nM rotenone or vehicle for 8 h. Images are representative photomicrographs immunostained for phosphorylated (p-) JNK and tyrosine hydroxylase (TH) (arrows), a marker for dopamine neurons. Scale bar: 20 μm. (B) TH^+ dopaminergic neurons from $JNK3^{-/-}$ mice exhibit resistance to rotenone toxicity. $Jnk3^{+/-}$ mice were mated and primary mesencephalic neurons were cultured separately from each mouse E14 fetus for 6 days. Cells were then treated with 5 nM rotenone for 24 h. (C, D) Ectopic expression of JNK3 induces cell loss. Mesencephalic cultures, prepared from E14 C57BL/6 mouse embryos, were co-transfected with plasmids encoding GFP and JNK3 cDNA or empty vector. Transfected cells were identified by GFP autofluorescence (arrows) 48 h later (C), and the total number of GFP^+ cells on each coverslip (9mm diameter) was quantified and presented as cell number / area. (D).

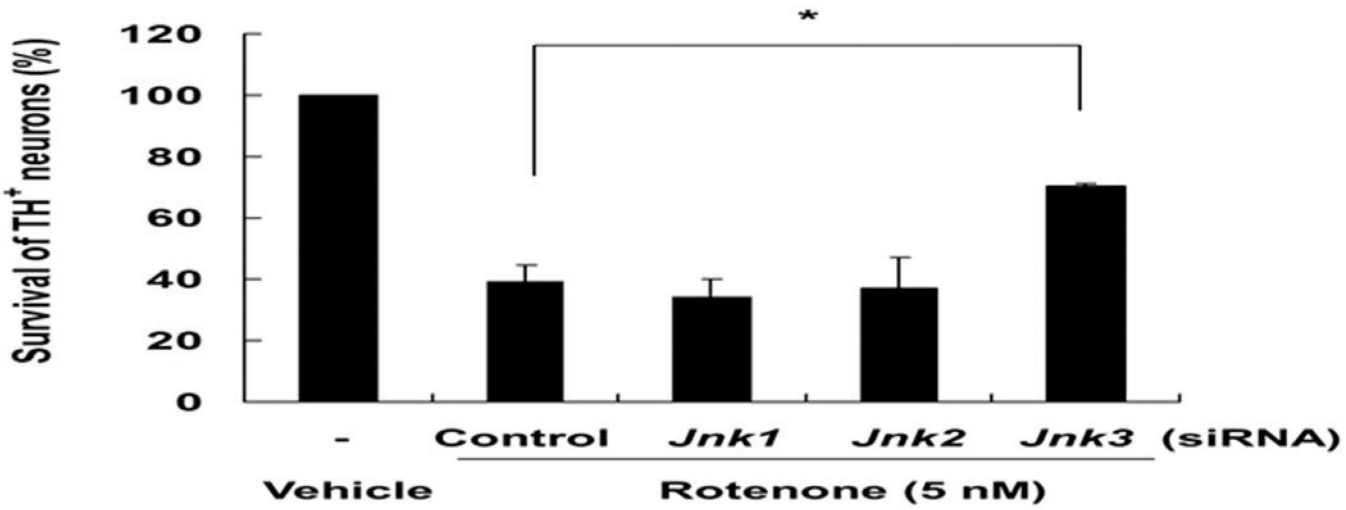

Fig. 2. siRNA targeting JNK3, but not JNK1 or JNK2, attenuates rotenone-induced dopaminergic neuron death

Twenty-four hours after transfection of siRNA, E14 mesencephalic cultures were treated with 5 nM rotenone for 24 h. The number of TH^+ cells was quantified.

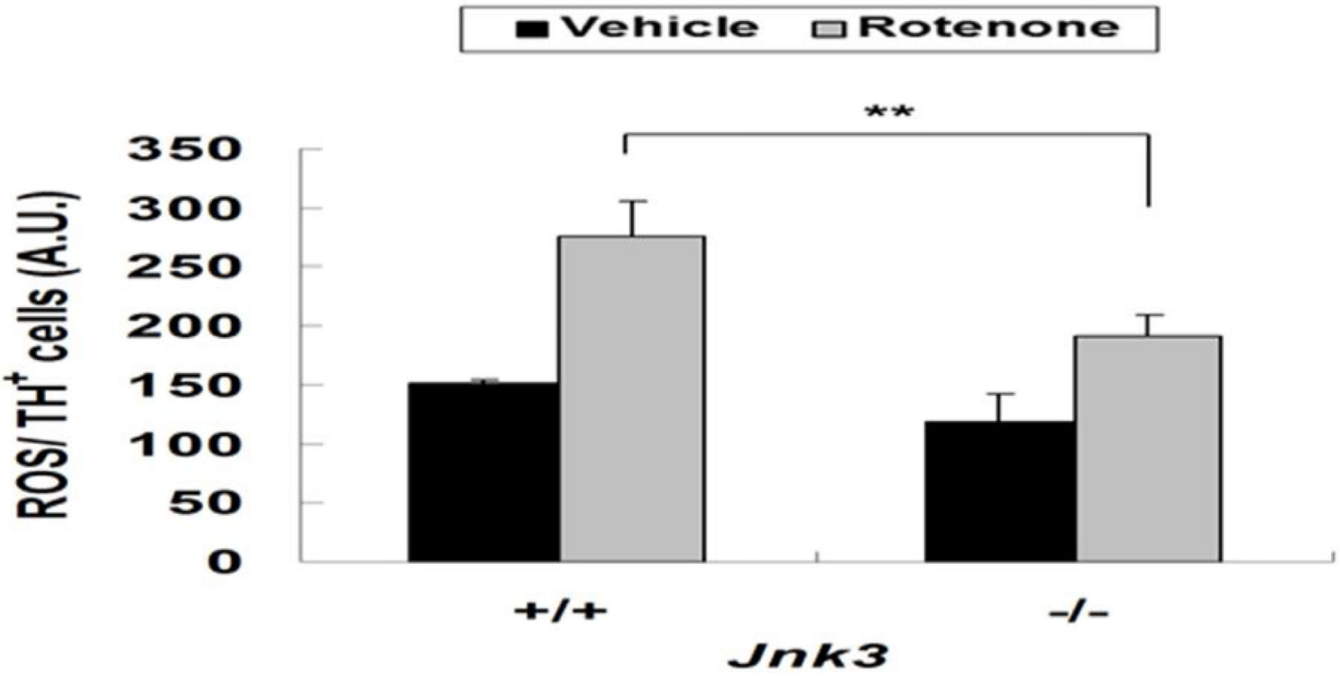

Fig. 3. *Jnk3* deletion attenuates ROS accumulation in dopamine neurons treated with rotenone

E14 mesencephalic cultures were treated with 5 nM rotenone or vehicle control on DIV 6. After 12 h, live cells were stained with CM-DCFDA to monitor ROS levels, photographed, then fixed and immunostained for TH for analysis. Images of CM-DCFDA and TH staining were superimposed. Cells stained positive for both were identified; the relative intensity of CM-DCFDA staining in TH^+ cells was quantified.

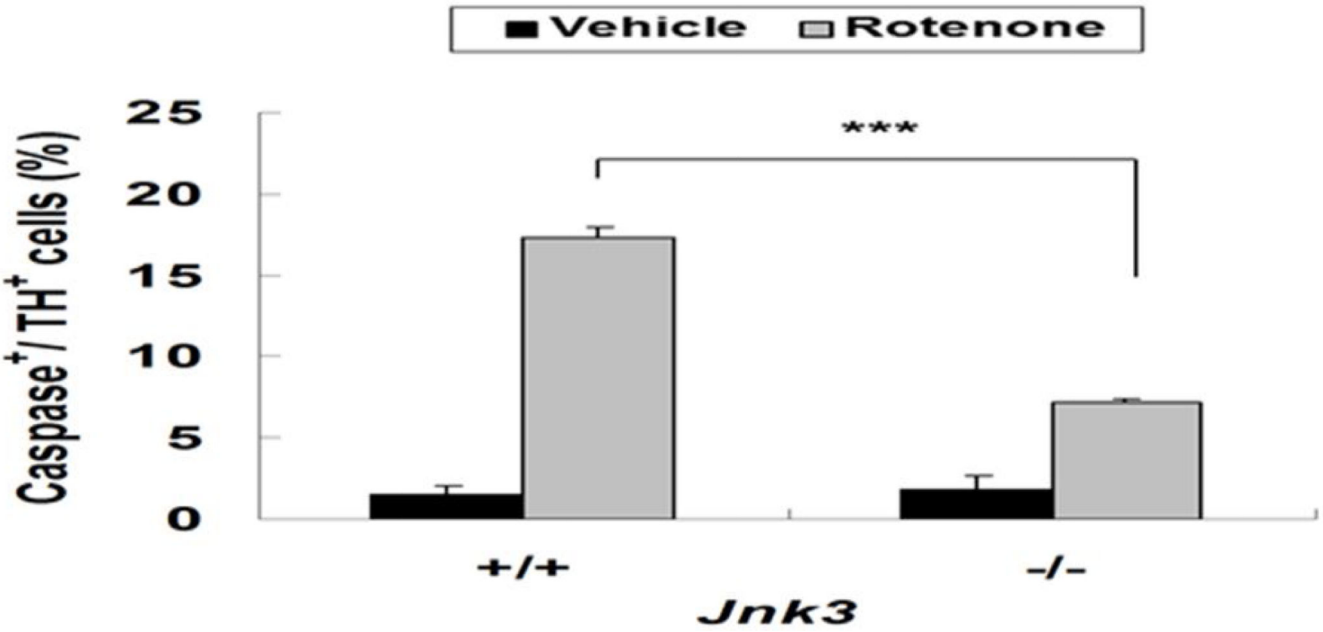

Fig. 4. *Jnk3* deletion reduces rotenone-induced caspase activation in TH^+ neurons

E14 mesencephalic cultures were treated with 5 nM rotenone or vehicle control on DIV 6 for 12h. Cells were fixed and immunostained for active caspase and TH. The number of caspase 3^+ cells among TH^+ cells was quantified.

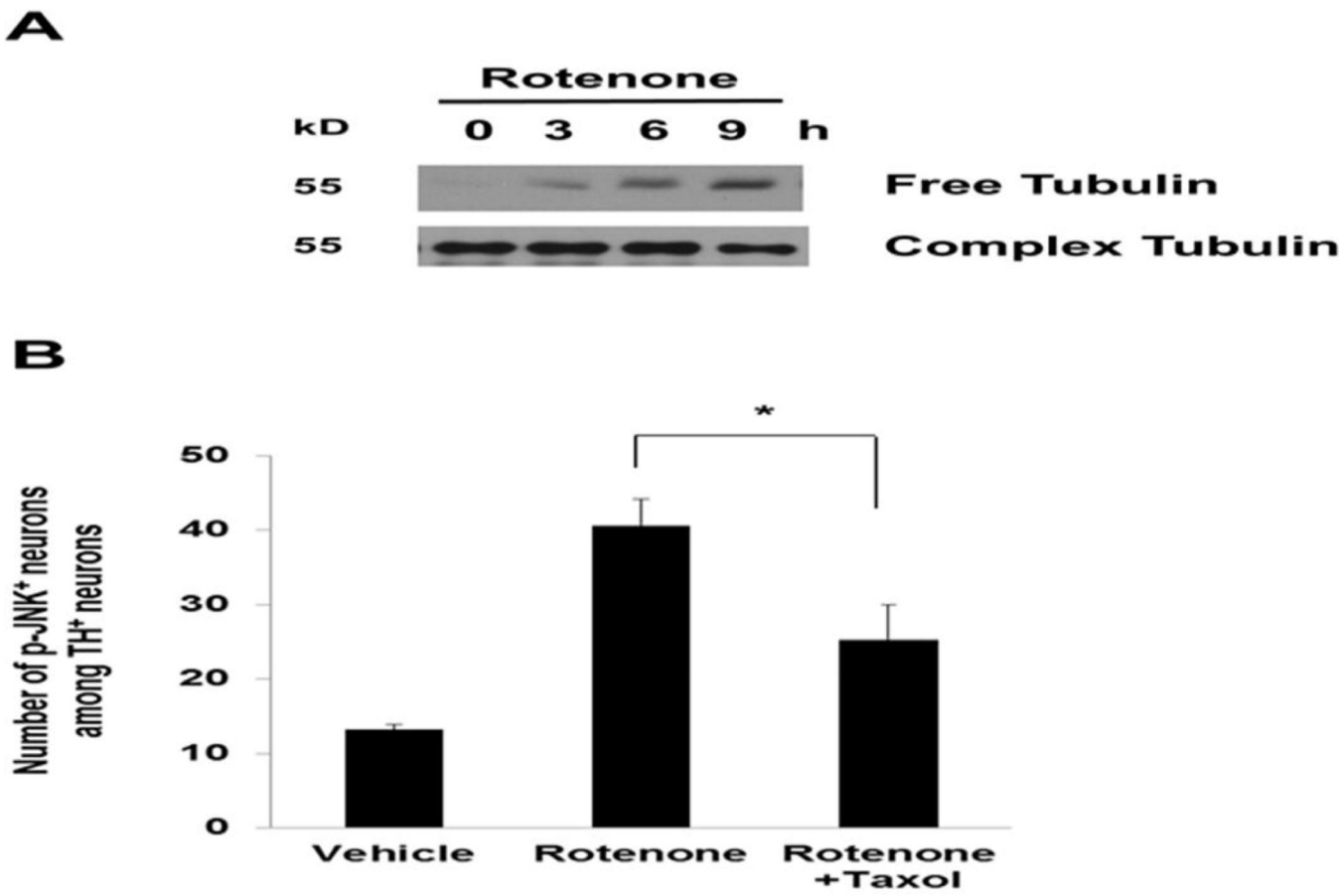

Fig. 5. Rotenone-induced microtubule de-polymerization activates JNK

(A) Accumulation of free tubulin after rotenone treatment, indicative of microtubule destabilization. E14 mesencephalic cultures were treated with 5 nM rotenone for 0, 3, 6, or 9 h. Cell lysates were prepared for Western analysis. (B) Taxol attenuates rotenone-induced JNK phosphorylation, an indicator of JNK activation. E14 mesencephalic cultures were co-treated with 5 nM rotenone and 10 nM taxol and for 8 h. Immunostaining was performed using anti-TH and anti-phospho-JNK (p-JNK) antibodies.

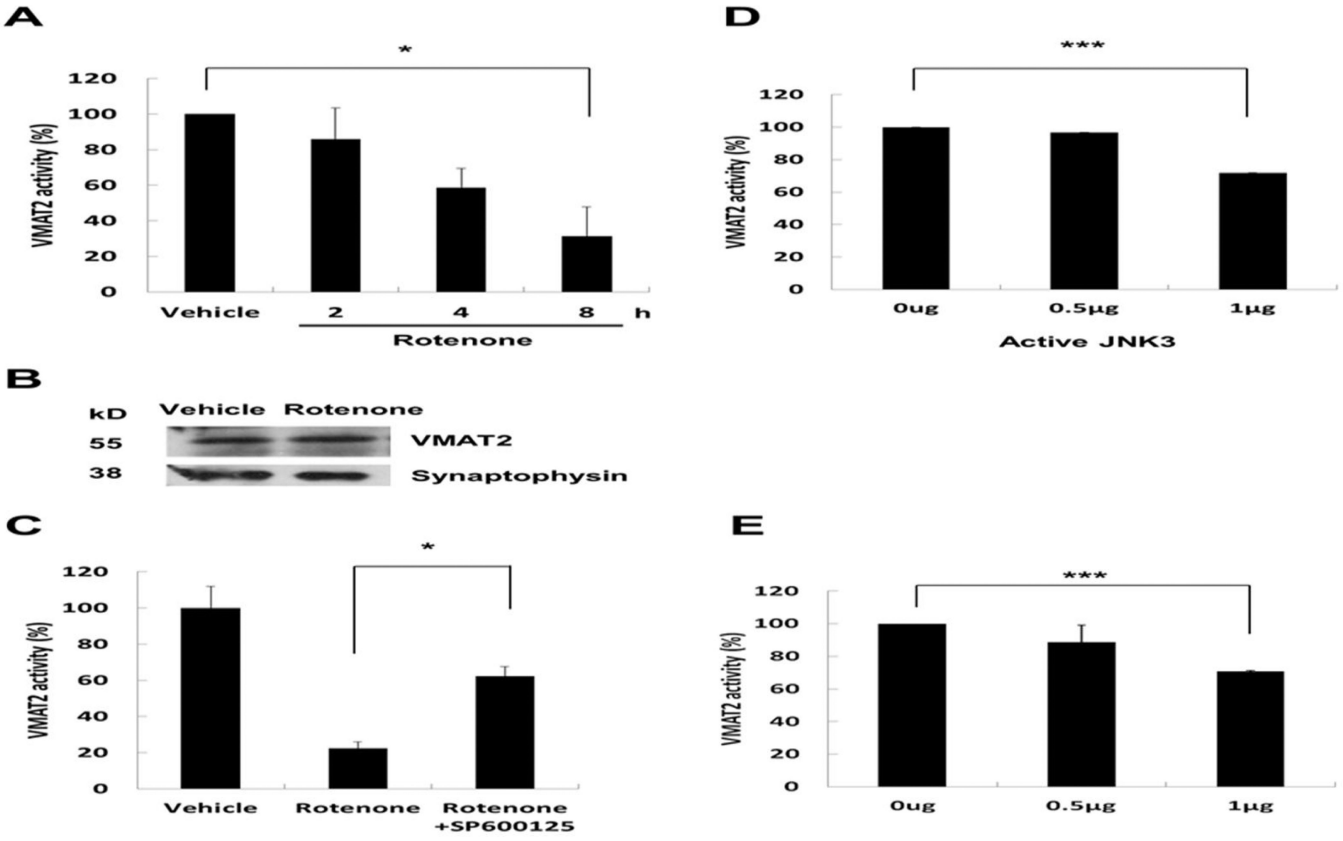

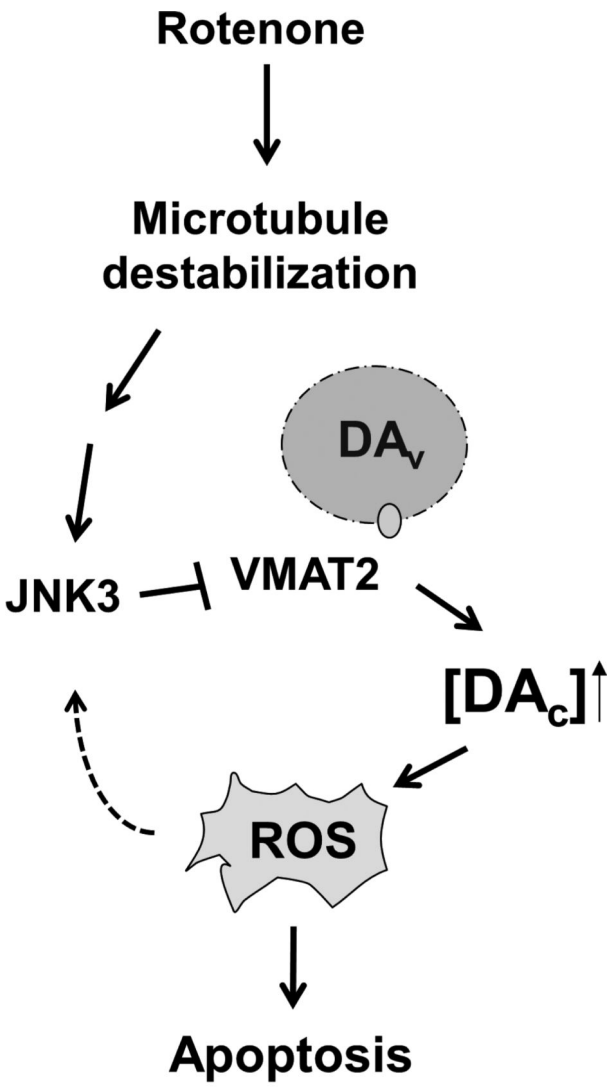

F

Fig. 6. Rotenone inhibits VMAT2 activity, which is mediated by JNK

(A) Rotenone inhibits VMAT2 activity. SH-SY5Y cells were incubated with 100 nM rotenone for 0–8 h. Synaptic vesicles were purified and VMAT2 activity was calculated as the uptake of [3H]dopamine (pmol) / synaptic vesicle (mg) / min. VMAT2 activity was presented as percent control. (B) Rotenone does not affect the level of VMAT2 protein. SH-SY5Y cells were incubated with 100 nM rotenone for 8 h. Total cell lysates were prepared for Western analysis. (C) Inhibition of JNK attenuates rotenone suppression of VMAT2. SH-SY5Y cells were pretreated with 10 μM SP600125 or vehicle for 1h, followed by

incubation with 100 nM rotenone or corresponding vehicle control for an additional 8 h. Synaptic vesicles were purified and VMAT2 activity was assayed. (D). JNK3 inhibition of VMAT2 activity in an *in vitro* reconstituted system. Synaptic vesicles were purified from the striatum of C57BL/6 mice and incubated with purified, active form of recombinant JNK3 protein for 1 h before VMAT2 activity was measured. (E). JNK3 inhibition of VMAT2 activity in an *in vitro* reconstituted system using synaptic vesicles purified from primary dopaminergic neurons. (F). Schematic diagram to illustrate our findings and current working hypothesis. DA_v, Vesicular dopamine; DA_c, cytosolic dopamine.